RSC Advances

PAPER

View Article Online
View Journal | View Issue

Cite this: *RSC Adv.*, 2021, **11**, 15565

N-Hydroxysuccinimide crosslinked graphene oxide–gold nanoflower modified SPE electrode for sensitive detection of chloramphenicol antibiotic

M. R. Ali,[ab] M. S. Bacchu,[ab] M. R. Al-Mamun,[ab] M. S. Ahommed,[c] M. Aly Saad Aly[d] and M. Z. H. Khan *[ab]

Received 28th March 2021
Accepted 21st April 2021

DOI: 10.1039/d1ra02450g

rsc.li/rsc-advances

Here we introduce a composite material that consists of graphene oxide (GO) sheets crosslinked with *N*-hydroxysuccinimide (NHS) and functionalized with gold nanoflowers (AuNFs). Furthermore, a screen printed electrode (SPE) modified with the introduced composite is electrochemically reduced to obtain an SPE/rGO–NHS–AuNFs electrode for sensitive and selective determination of chloramphenicol (CAP) antibiotic drug. The morphological structure of the as-prepared nanocomposite was characterized by scanning electron microscopy, energy-dispersive X-ray spectroscopy, cyclic voltammetry, Fourier-transform infrared spectroscopy and electrochemical impedance spectroscopy. The proposed sensor demonstrated excellent performance with a linear concentration range of 0.05 to 100 μM and a detection limit of 1 nM. The proposed electrode offers a high level of selectivity, stability, reproducibility and a satisfactory recovery rate for electrochemical detection of CAP in real samples such as blood serum, poultry feed, milk, eggs, honey and powdered milk samples. This further demonstrates the practical feasibility of the proposed sensor in food analysis.

1. Introduction

The presence of different harmful biological substances in food and the body is rapidly increasing, thus it becomes vital to detect specific molecules or substances at a low concentration level. This concern pushes researchers worldwide to develop rapid, inexpensive and precise detection methods for food contaminants to ensure food safety. Chloramphenicol (CAP) is a bacteriostatic agent commonly used as a low-priced broad-spectrum antibiotic that was also effective against Gram-positive and Gram-negative bacteria.[1] The initial drug discovery of CAP aimed to treat infectious diseases like plague, cholera, typhoid fever and meningitis.[2,3] Later, research efforts revealed that CAP had severe side-effects on human beings due to toxicity that was shown to cause reversible bone marrow suppression, irreversible aplastic anemia, leukemia and gray baby syndrome.[4,5] As chloramphenicol can easily enter the human body upon intake from medicines and foods, many developed countries prohibited CAP for treating food-producing animals under food safety protocols. However, due to the low-cost availability and high efficacy rate, it is still used in many developing countries.[6] Thus, a susceptible and selective method to detect CAP is becoming crucial.

Different analytical methods were performed to detect chloramphenicol including high-performance liquid chromatography (HPLC),[7] gas chromatography-mass spectrometry (GC-MS),[8] Raman scattering,[9] antibody-based techniques,[10] chemiluminescence[11] and electrochemical techniques.[12] Recently, electrochemical detection of CAP was considered the most promising strategy because of several advantages, such as the simplicity of operation, portability of equipment, affordability of cost, rapidity of response, and high sensitivity and selectivity compared to other methods.[13] However, the overall response of the electrochemical sensing system highly depends on the electrode materials.[14,15] Various electrode materials were applied for CAP detection such as single-wall carbon nanotube–AuNPs composites,[16] MoS_2/polyaniline (PANI) composites,[17] cadmium sulfide nanoparticles modified-dendrimer.[18] Furthermore, reduced GO incorporating with different nanoparticles showed excellent outcome for chloramphenicol detection.[19,20] Reduced graphene oxide (rGO) has been widely used in electrochemical sensors because of their graphene-like properties and ease of fabrication.[21] Being a two-dimensional sp^2 hybridized nanocarbon material, rGO provides superior electrical conductivity, high electrocatalytic activity, good mechanical stability and high sensitivity towards sensing mechanism.[22] For these reasons, rGo has been utilized in

[a]*Dept of Chemical Engineering, Jashore University of Science and Technology, Jashore, 7408, Bangladesh. E-mail: zaved.khan@just.edu.bd*

[b]*Laboratory of Nano-bio and Advanced Materials Engineering (NAME), Jashore University of Science and Technology, Jashore, 7408, Bangladesh*

[c]*Department of Chemistry, Graduate School of Science, Tohoku University, Aoba-ku, Sendai 980-8578, Japan*

[d]*Department of Electronics and Information Science, Miami College of Henan University, Kaifeng 475000, China*

electrochemical sensors including voltametric,[23] potentiometric,[24] amperometric,[25] electrochemical impedance spectroscopy technique[26] and more focus on rGO/nanoparticles composites for sensing strategy were observed.[27] Yadav *et al.* developed cobalt oxide decorated reduced graphene oxide sheets (Co_3O_4@rGO) to detect CAP and achieved a linear range of 1–2000 μM with sensitivity of 1.32 μA μM cm^{-2}.[28] Palladium nanoparticles were successfully decorated with rGO to detect CAP with a low detection limit of 50 nM as reported by Yi *et al.*[26] Additionally, they demonstrated the significant role of rGO as an active material for the electrode modification process in detecting chloramphenicol. Govindasamy *et al.* prepared rGO@Cu_2S nanocomposites by following ultra-sonicated method obtaining a lower charge-transfer resistance at the electrode surface for real monitoring of CAP in food sample at nanomolar level.[29] Besides, some reports showed that *N*-hydroxysuccinimide (NHS) can be used as a key reagent to activate the carboxylic acid group (–COOH) of rGO by intensifying electrochemical reaction.[30,31]

Conductive metallic nanomaterials attracted the attention of numerous scientists and research groups in the field of nanoscience and nanotechnology. Particularly, gold nanoparticles (AuNPs) were broadly studied owing to their extended surface functionalities, electrical, optical and excellent catalytic properties. Especially in the electrochemical sensing research area, Au nanoparticles got more attention due to their high chemical stability and biological compatibility.[32] However, properties of AuNPs can be controlled by modifying their size, shapes and supporting materials. In view of this, researchers synthesized AuNPs with different sizes and shapes such as spherical,[33] triangular,[34] cubic,[35] nanorod[36] and nanoflowers[37] by following different synthetic methods. Compared with other shapes of AuNPs, gold nanoflowers (AuNFs) provide more surface-to-volume ratio that enhances the electrocatalytic performance of the sensors.[38] Functional nanomaterials can amplify the signal of the electrochemical sensor due to their enhanced electrochemical properties, ensuring high sensitivity.[39,40] Based on comprehensive research, it was proven that the application of AuNFs in electrochemical sensors increased the electron transfer rate and sensitivity of sensors.[41,42]

In this study, GO–NHS–AuNFs nanocomposite was successfully prepared by crosslinking GO nanosheets with NHS ester and decorated with AuNFs. Later, the modified electrode was characterized by various analytical and spectroscopic methods. In addition, the modified electrode was used as an electrochemical sensing platform to detect chloramphenicol by differential pulse voltammetry method. Finally, the analytical performance of the proposed sensor was tested to detect CAP in various commercial real samples.

2. Materials and methods

2.1 Reagents

Tetrachloroauric acid ($HAuCl_4$), ascorbic acid (AA), graphene oxide (GO), *N*-hydroxysuccinimide (NHS) and sliver nitrate ($AgNO_3$) were purchased from Sigma Aldrich (City, China). Cetrimonium bromide (CTAB) was bought from Merck (City, India). Chloramphenicol was supplied by local pharmaceuticals company. All type of solution were made by using ultrapure water (type-I) which was obtained from Evoqua (Germany, resistivity > 18 MΩ cm). A phosphate buffer saline of 0.01 M was used as a supporting electrolytic solution for all voltammetric experiments. Nitrogen gas (N_2) was used as an inert atmosphere before all voltammetric runs.

2.2 Apparatus

A CS300 electrochemical workstation (Corrtest, Wuhan, China) was employed to conduct all electrochemical measurements. A Metrohms (DropSens) screen-printed electrode (SPE, 110), three-electrode system, was used to execute the voltammetric studies. Working and auxiliary electrodes were made of carbon, while reference electrode was available in silver or silver/silver chloride. The surface morphologies of different modified electrodes were investigated using ZEISS Gemini SEM 500 scanning electron microscope (SEM) equipped with BRUKER energy disperse X-ray spectrophotometer with an accelerating voltage of 5–20 kV. Thermo scientific ATR-FTIR (Model: Smart iTR) was used to take Fourier transform infrared (FTIR) absorption spectra. UV-vis experiment was done with Shimadzu UV1900 model. For UV experiment, 1 mL GO–NHS–AuNFs nanocomposite solution contains 0.2 mg GO, 2 mM NHS and 100 μL as-prepared AUNFs.

2.3 Preparation of gold nanoflowers (AuNFs)

About 5 μL of 3 M $HAuCl_4$ solution was added into 15 mL of 200 mM CTAB aqueous solution. The prepared solution was continuously stirred at 600 rpm for 3 minutes, 300 μL of 10 mM $AgNO_3$ was added and the mixture was stirred for extra 3 minutes. Next, 0.75 mL of 0.3 M AA was added to the mixture and was stirred for another 3 minutes. Following, the mixture was left for 4 minutes at room temperature and then was refrigerated for 5 hours. The obtained AuNFs were centrifuged at 5000 rpm for 5 minutes to remove the excess surfactants and then washed several times with ethanol and ultrapure water. Finally, the residue was stored in 3 mL of ultrapure water.

2.4 Preparation of the SPE/rGO–NHS–AuNFs

A 1 mg of graphene oxide (GO) powder was dispersed in 1 mL of phosphate buffer saline (PBS, pH 7.4) and the mixture was ultrasonicated for 20 minutes followed by 5 minutes of stirring in order to get a homogenous solution. Next, 100 μL of previously synthesized AuNFs and 10 mM NHS were mixed with GO solution and then the mixture was further ultrasonicated for 10 minutes. The SPE/rGO–NHS–AuNFs was prepared by drop-casting a 10 μL aliquot of the solution, drying on air and followed by electrochemical reduction *via* cyclic voltammetry at a voltammetric range of −1.4 V to 0.7 V with a scan rate of 100 mV s^{-1} for 10 cycles.

2.5 Electrochemical measurement

Electrochemical determination of CAP was performed through differential pulse voltammetry (DPV) in 0.01 M PBS solution.

The DPV parameters were set at initial potential of −0.3 V, end potential of −0.75 V, pulse width of 50 ms, modulation amplitude of 50 mV and pulse period of 0.1 s.

2.6 Real sample preparation

Real sample analysis was carried out using blood serum, urine and some commercially available samples. Egg, milk and honey samples were prepared by the same procedure. A 1.00 g of each sample and 3.0 mL of 10% trichloroacetic acid were added into a 15 mL polypropylene centrifuge tube. In order to produce a homogenous mixture, it was vortexed and ultrasonicated for 1 minute and 5 minutes, respectively. Next, the mixture was centrifuged for 10 minutes at 3500 rpm, the supernatant was separated by filter paper and diluted 200 times using 0.1 mM PBS (pH 7.4) following the procedure reported by Hu *et al.*[43]

For poultry feed, a 2.00 g of feed and 2.0 mL ultrapure water were added into a 15 mL polypropylene centrifuge tube and vortexed for 1 minute. Next, 4 mL of ethyl acetate was added into the mixture and ultrasonicated for 5 minutes. The mixture was centrifuged at 5000 rpm for 10 minutes, supernatant was filtrated and was completely dried at 50 °C following the procedure reported by Bakar *et al.*[44]

3. Results and discussion

3.1 Morphology and microstructures of prepared nanocomposite

The surface morphology of the as-prepared nanocomposites was characterized by field emission scanning electron microscope (FE-SEM) as shown in Fig. 1. In multilayer GO nanosheet, in which the graphitic material displayed a typical wrinkled structure with plenty of corrugations is shown in Fig. 1A. The size of supplied single GO sheet was 5–20 μm with a thickness of about 0.9 nm. AuNFs with Au displaying a 3D flower-like morphology and an average size of 100–300 nm is shown in Fig. 1B. The magnified view of the prepared rGO–NHS–AuNFs nanocomposite presented in Fig. 1C revealed the incorporation and strong interaction between AuNFs and the reduced graphene oxide (rGO) through covalent bond. Energy dispersive X-ray analysis (EDX) data (Fig. 1D) of rGO–NHS–AuNFs showed that rGO sheets were decorated with AuNFs. The EDX plane distributions of the typical elements on the nanocomposite surface confirmed the presence of elements C, O and Au as shown in Fig. 1E–G.

Fig. 2A shows the typical attenuated total reflectance Fourier transform infrared spectroscopy (ATR-FTIR) spectrum obtained for prepared nanocomposite. FTIR spectra analysis showed intense bands at 1606 cm^{-1} suggest the presence of stretching vibrations (N–H) in gold nanoparticles as reported by earlier researchers.[45] The characteristic features in the ATR-FTIR spectrum of GO-NHS are the absorption bands corresponding to the C=C vibrations at 1676 cm^{-1}, the C–O stretching at 1227 cm^{-1} and 1030 cm^{-1} respectively. The small spectrum band around 1722 cm^{-1} may be observed for C=O. Finally, the intense band observed at 3367 cm^{-1} shows O–H stretching vibration.

The formation of synthesized AuNFs further confirmed by UV-vis spectra (Fig. 2B) where a strong and broad peak around at 523 nm attributed to the localized surface plasmon resonance of gold nanoparticle. The analysis of the GO-NHS spectrum reveals that the absorption peak at 265 nm which demonstrates the occurrence of crosslinking within the graphene sheets through NHS ester. Moreover, the absorption peaks obtained for GO–NHS–AuNFs at 231 and 535 nm demonstrates the incorporation of AuNFs on the GO-NHS composite as reported by earlier researcher.[46] As the conjugation in the Π-bond increases, the absorption peak shift to the longer wavelength region.

3.2 Electrochemical characteristics of SPE/rGO–NHS–AuNFs

The electrochemical characteristics of different modified electrodes were investigated *via* cyclic voltammograms (CVs) in

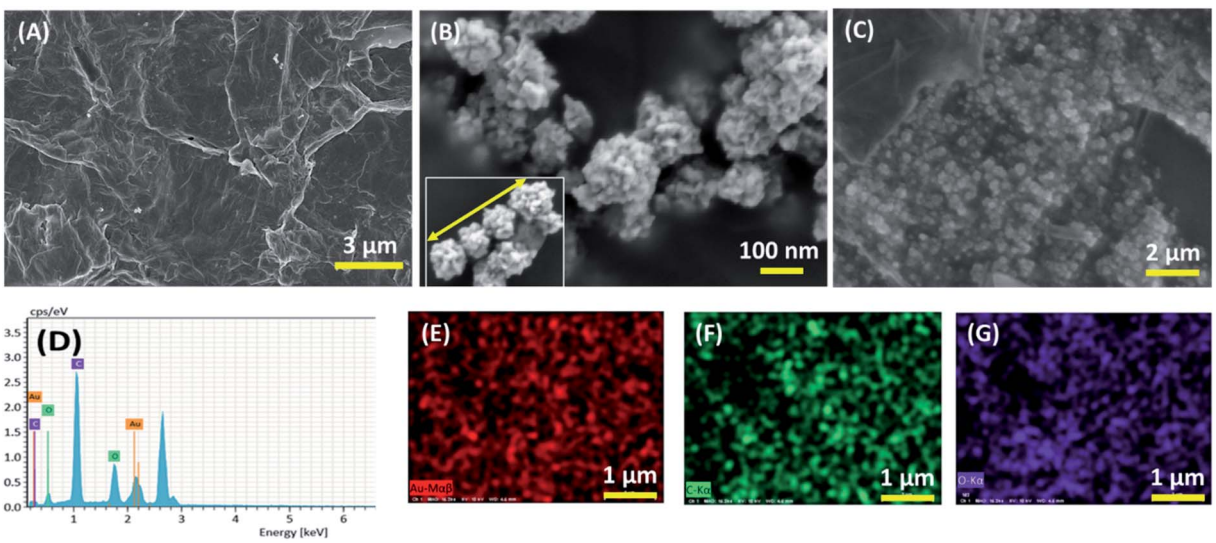

Fig. 1 SEM images of (A) GO; (B) as-prepared AuNFs; and (C) rGO–NHS–AuNFs. Results of the EDX element analysis of rGO–NHS–AuNFs (D). EDX mapping images (E–G) of sample where the bright spots show the distribution of C, O and Au elements on the rGO–NHS–AuNFs surface.

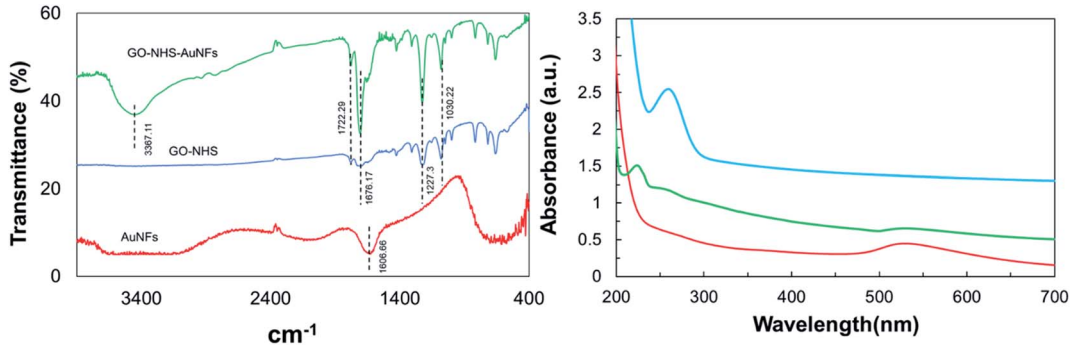

Fig. 2 ATR-FTIR spectrum (A) and UV-vis absorption spectra (B) obtained for AuNFs, GO-NHS, and GO–NHS–AuNFs nanocomposite.

which $[Fe(CN)_6]^{3-/4-}$ was chosen as a redox probe for this analysis. The CV of different electrodes in 0.1 M KCl solution containing 5 mM of the redox probe at a scan rate of 100 mV s^{-1} is shown in Fig. 3A. The peak-to-peak separation values ($\Delta E_p = E_{pc} - E_{pa}$) of bare SPE is calculated as 130 mV, indicating a slow electron transfer kinetics of SPE. After the modification of rGO, rGO-NHS and rGO–NHS–AuNFs on the surface of SPE, the peak-to-peak separation values became smaller. The difference of anodic and cathodic peak position of SPE/rGO–NHS–AuNFs ($\Delta E_p = 71$ mV) is less than that of SPE/rGO ($\Delta E_p = 85$ mV) and SPE/rGO-NHS ($\Delta E_p = 78$ mV) and that indicates that SPE/rGO–NHS–AuNFs exhibits faster electron transfer kinetics and higher electroactivity than other electrodes.[47]

The effect of the scan rate on the potential response of the proposed sensor was confirmed by a series of CVs analysis of 100 μM CAP at different scan rate of 10, 20, 30, 40, 50, 60, 70, 80, 90, 100, 150 and 200 mV s^{-1} in potential range of −0.15 V to −0.75 V, as shown in Fig. 3B. The linear ($R^2 = 0.9932$) relationship between the scan rate and reduction peak current depicted in Fig. 3B suggests adsorption controlled behavior of CAP on the surface of SPE/rGO–NHS–AuNFs.[48]

3.3 Electrochemical detection of CAP

DPV technique was used to analyze the analytical performance of different modified electrodes in 100 μM CAP containing 0.01 M PBS. The reduction peak was increased after the introduction of rGO–NHS–AuNFs on the surface of SPE as show in Fig. 4A. This result indicates that the electroactivity of SPE was enhanced when AuNFs were supported with the conductive layer GO-NHS on the surface of SPE.

Under some optimized condition, a series of DPV analysis was performed to detect CAP in 0.01 M PBS by using SPE/rGO–NHS–AuNFs. The measurement expressed the reduction peak potential that was gradually enhanced with increasing the concentration of CAP and exhibited an excellent linear relationship between the concentration range of 0.05–100 μM ($R^2 = 0.995$). The proposed electrochemical sensor had lower detection limit (LOD) of 0.001 μM, which is much lower than previously reported electrochemical investigations for the CAP detection as summarized in Table 1.

3.4 Selectivity, reproducibility, and stability of the SPE/rGO–NHS–AuNFs electrode

Selectivity, reproducibility, and stability are the most important parameters for evaluating the performance of the modified electrode. To assess the selectivity of the modified SPE/rGO–NHS–AuNFs for the detection of CAP, it was carried out with various interfering ions (Ca^{2+}, Mg^{2+}, Na^+, K^+, Fe^{2+}, Fe^{3+}, Cl^-, Al^{3+}, NO_3^-, SO_4^{2-}) and organic compounds such as ascorbic acid and uric acid. The current responses were observed with the addition of those common interfering substances in the presence of 0.01 M PBS (pH of 7.4) solution. It can be seen that

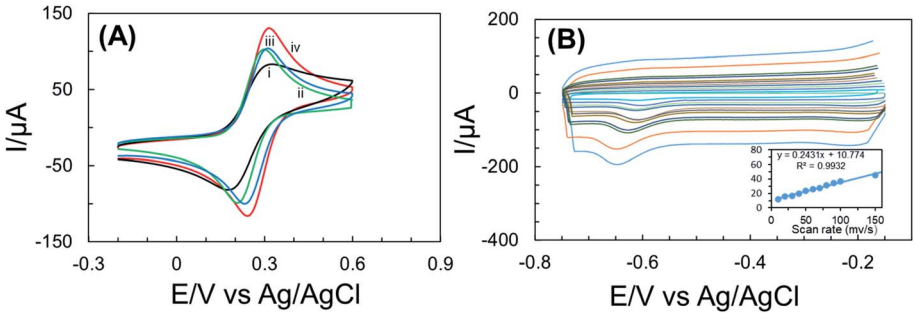

Fig. 3 Cyclic voltammograms (A) of the different electrodes measured in 0.1 mol L^{-1} KCl including 5.0×10^{-3} mol L^{-1} $Fe(CN)_6^{3-/4-}$: (i) bare SPE, (ii) SPE/rGO, (iii) SPE/rGO-NHS and (iv) SPE/rGO–NHS–AuNFs. CV response obtained for SPE/rGO–AuNFs-NHS sensor at different scan rates (from inner to outer): 10, 20, 30, 40, 50, 60, 70, 80, 90, 100, 150 and 200 mV s^{-1} in 0.01 mol L^{-1} PBS including 1.0×10^{-3} mol L^{-1} CAP solution (B). All potentials are given *vs.* Ag/AgCl. The inset shows the dependence of the peak currents on the scan rates.

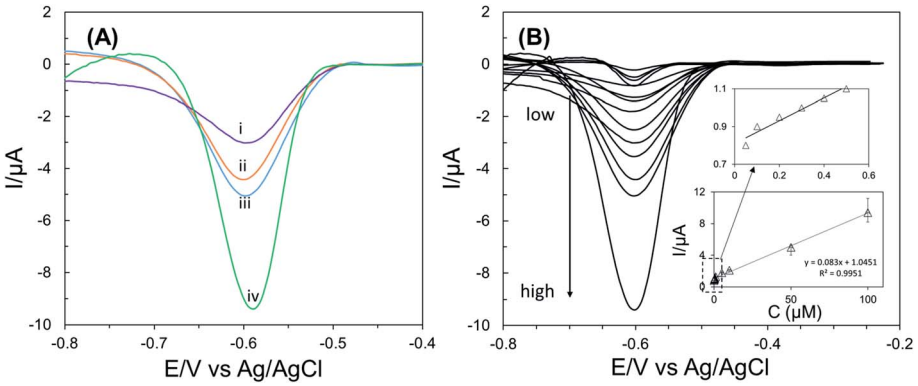

Fig. 4 (A) DPVs of 1×10^{-3} mol L^{-1} CAP at (i) bare SPE, (ii) SPE/rGO, (iii) SPE/rGO-NHS and (iv) SPE/rGO–NHS–AuNFs in phosphate buffer (7.4 pH) at a scan rate of 100 mV s^{-1}. (B) DPVs obtained for the detection of CAP using SPE/rGO–NHS–AuNFs sensor in phosphate buffer (7.4 pH) at scan rate of 100 mV s^{-1} with a wide range of concentrations from 0.05 μM to 100 μM. The inset shows the calibration curves for all concentrations.

the oxidation response of CAP with the addition of all interfering substances remains unchanged (<3%) and that indicates that the proposed electrode has an acceptable working selectivity.

To study the reproducibility of the SPE/rGO–NHS–AuNFs electrode, a series of repetitive DPV experiments were performed using the same electrode. Less than 1% deviation of current response for various concentrations of samples was observed and that indicates that SPE/rGO–NHS–AuNFs electrode had an excellent reproducibility.

Furthermore, the stability of SPE/rGO–NHS–AuNFs was employed under the optimized conditions of DPV and was recorded for CAP (100 μM) in 0.1 M PBS (pH = 7.4) at 100 mV s^{-1}. The DPV response of CAP was examined over 14 days and was checked every 7 days while being stored in a refrigerator at 4 °C. There was no significant deviation in the peak response (1.56%) found after 7 days of storage. In comparison, a small deviation of the peak response (4.11%) was found after the 14 days of storage and that suggests that the proposed sensor has an excellent stability and lifetime. However, the proposed electrode has potential selectivity, reproducibility, and stability for CAP detection.

3.5 Real sample analysis

To evaluate the analytical reliability of the proposed modified sensor, it was tested with commercially available real samples. The modified electrode was used with the actual real samples such as poultry feeds, blood serum, milk, honey and egg to

Table 1 Detection limit and linear dynamic range of various methods for determination of CAP

Electrode	Method	Linear range (μM)	LOD (μM)	Ref.
rGO/PdNPs	DPV	0.50–1	0.05	49
Gr/CuPc	DPV	1–30	0.75	50
AuNPs/GO	Amperometry	1.5–2.95	0.25	51
Fe_3O_4/GCE	SWV	0.09–47	0.09	52
Si–Fe/NOMC	DPV	1–500	0.03	53
MoS_2-IL/GO	DPV	0.1–400	0.047	54
MoS_2/*f*-MWCNTs	Amperometry	0.08–1392	0.015	55
SPE/rGO–NHS–AuNFs	DPV	0.05–100	0.001	This work

Table 2 Detection of CAP in different real samples at SPE/rGO–NHS–AuNFs electrode

Sample	Added (μM)	Found (μM)	Relative recovery (%)	RSD (%) ($n = 3$)
Commercial poultry feed	100	101.1	101.1	2.30
Blood serum	100	95.7	95.7	3.26
Milk	100	95.6	95.6	2.42
Honey	100	101.8	101.8	2.27
Egg	100	103.3	103.3	2.63

evaluate the electrochemical detection of CAP quantitatively. The real samples were collected from a local market and the preparation technique was followed by the standard method as stated in the methodology section. The DPV was formulated using SPE/rGO–NHS–AuNFs electrode and a known concentration of CAP was spiked into the PBS with an appropriate time interval. The obtained recovery values of CAP sensing the real samples with the addition of standard approach method were summarized in Table 2. The proposed modified sensor displayed satisfactory recovery results ranged from 95.6% to 103.3%, and the relative standard deviation (RSD) was less than 4.0% ($n = 3$). The obtained results suggest potential reliability for the rapid and sensitive detection of CAP in real samples.

4. Conclusion

In summary, a highly selective and sensitive rGO–NHS–AuNFs nanocomposite modified screen-printed electrode-based CAP sensor was developed. *N*-Hydroxysuccinimide acted as a cross-linking agent to deposit multilayer graphene oxide sheets. The proposed electrode exhibited an enhanced differential pulse voltammetry response to CAP with high selectivity, wide linear range, excellent sensitivity with a LOD of 1 nM. The application of the proposed sensor was demonstrated with different real food samples, including human blood serum and satisfactory recovery results were obtained. The present findings indicate that rGO–NHS–AuNFs nanocomposite modified SPE electrode hold high promise in food safety analysis.

Conflicts of interest

The authors declare that there is no conflict of interest in this work.

Acknowledgements

The work has been done with the financial support from the Ministry of Information and Communication Technology, Government of Bangladesh (Innovation Fund).

References

1 S.-P. Ho, T.-Y. Hsu, M.-H. Chen and W.-S. Wang, Antibacterial Effect of Chloramphenicol, Thiamphenicol and Florfenicol against Aquatic Animal Bacteria, *J. Vet. Med. Sci.*, 2000, **62**, 479–485, DOI: 10.1292/jvms.62.479.

2 M. D. L. A. Del Rio, S. Shelton, D. Chrane, G. H. Mccracken and J. D. Nelson, Ceftriaxone *versus* Ampicillin and Chloramphenicol for Treatment of Bacterial Meningitis in Children, *Lancet*, 1983, **321**, 1241–1244, DOI: 10.1016/S0140-6736(83)92696-X.

3 A. Carcelen, J. Chirinos and A. Yi, Furazolidone and chloramphenicol for treatment of typhoid fever, *Scand. J. Gastroenterol.*, 1989, **24**, 19–23, DOI: 10.3109/00365528909091327.

4 M. E. Falagas, A. P. Grammatikos and A. Michalopoulos, Potential of old-generation antibiotics to address current need for new antibiotics, *Expert Rev. Anti-Infect. Ther.*, 2008, **6**, 593–600, DOI: 10.1586/14787210.6.5.593.

5 J. C. Hanekamp and A. Bast, Antibiotics exposure and health risks: Chloramphenicol, *Environ. Toxicol. Pharmacol.*, 2015, **39**, 213–220, DOI: 10.1016/j.etap.2014.11.016.

6 S. Sood, Chloramphenicol – A potent armament against multi-drug resistant (MDR) Gram negative bacilli?, *J. Clin. Diagn. Res.*, 2016, **10**, DC01–DC03, DOI: 10.7860/JCDR/2016/14989.7167.

7 N. Zhang, F. Xiao, J. Bai, Y. Lai, J. Hou, Y. Xian and L. Jin, Label-free immunoassay for chloramphenicol based on hollow gold nanospheres/chitosan composite, *Talanta*, 2011, **87**, 100–105, DOI: 10.1016/j.talanta.2011.07.108.

8 S. Impens, W. Reybroeck, J. Vercammen, D. Courtheyn, S. Ooghe, K. De Wasch, W. Smedts and H. De Brabander, Screening and confirmation of chloramphenicol in shrimp tissue using ELISA in combination with GC-MS2 and LC-MS2, *Anal. Chim. Acta*, 2003, **483**, 153–163, DOI: 10.1016/S0003-2670(02)01232-1.

9 W. Ji and W. Yao, Rapid surface enhanced Raman scattering detection method for chloramphenicol residues, *Spectrochim. Acta, Part A*, 2015, **144**, 125–130, DOI: 10.1016/j.saa.2015.02.029.

10 N. A. Karaseva and T. N. Ermolaeva, A piezoelectric immunosensor for chloramphenicol detection in food, *Talanta*, 2012, **93**, 44–48, DOI: 10.1016/j.talanta.2011.12.047.

11 X. Tao, H. Jiang, J. Zhu, X. Wang, Z. Wang, L. Niu, X. Wu, W. Shi and J. Shen, An ultrasensitive chemiluminescent ELISA for determination of chloramphenicol in milk, milk powder, honey, eggs and chicken muscle, *Food Agric. Immunol.*, 2014, **25**, 137–148, DOI: 10.1080/09540105.2012.753513.

12 Y. Zhuang, L. Cai and G. Cao, Determination of Chloramphenicol by Voltammetric Method, *J. Electrochem. Soc.*, 2014, **161**, H129–H132, DOI: 10.1149/2.058403jes.

13 M. Chen, N. Gan, H. Zhang, Z. Yan, T. Li, Y. Chen, Q. Xu and Q. Jiang, Electrochemical simultaneous assay of chloramphenicol and PCB72 using magnetic and aptamer-modified quantum dot-encoded dendritic nanotracers for signal amplification, *Microchim. Acta*, 2016, **183**, 1099–1106, DOI: 10.1007/s00604-015-1695-1.

14 H. Hou, K. M. Zeinu, S. Gao, B. Liu, J. Yang and J. Hu, Recent Advances and Perspective on Design and Synthesis of Electrode Materials for Electrochemical Sensing of Heavy Metals, *Energy Environ. Mater.*, 2018, **1**, 113–131, DOI: 10.1002/eem2.12011.

15 M. R. Ali, M. S. Bacchu, M. Daizy, C. Tarafder, M. S. Hossain, M. M. Rahman and M. Z. H. Khan, A highly sensitive poly-arginine based MIP as an electrochemical sensor for selective detection of dimetridazole, *Anal. Chim. Acta*, 2020, **1121**, 11–16, DOI: 10.1016/j.aca.2020.05.004.

16 F. Xiao, F. Zhao, J. Li, R. Yan, J. Yu and B. Zeng, Sensitive voltammetric determination of chloramphenicol by using single-wall carbon nanotube-gold nanoparticle-ionic liquid composite film modified glassy carbon electrodes, *Anal. Chim. Acta*, 2007, **596**, 79–85, DOI: 10.1016/j.aca.2007.05.053.

17 R. Yang, J. Zhao, M. Chen, T. Yang, S. Luo and K. Jiao, Electrocatalytic determination of chloramphenicol based on molybdenum disulfide nanosheets and self-doped polyaniline, *Talanta*, 2015, **131**, 619–623, DOI: 10.1016/j.talanta.2014.08.035.

18 D. M. Kima, M. A. Rahmanb, M. H. Do, C. Ban and Y. B. Shim, An amperometric chloramphenicol immunosensor based on cadmium sulfide nanoparticles modified-dendrimer bonded conducting polymer, *Biosens. Bioelectron.*, 2010, **25**, 1781–1788, DOI: 10.1016/j.bios.2009.12.024.

19 X. Zhang, Y. C. Zhang and J. W. Zhang, A highly selective electrochemical sensor for chloramphenicol based on three-dimensional reduced graphene oxide architectures, *Talanta*, 2016, **161**, 567–573, DOI: 10.1016/j.talanta.2016.09.013.

20 N. Sebastian, W. C. Yu and D. Balram, Electrochemical detection of an antibiotic drug chloramphenicol based on a graphene oxide/hierarchical zinc oxide nanocomposite, *Inorg. Chem. Front.*, 2019, **6**, 82–93, DOI: 10.1039/c8qi01000e.

21 A. T. Smith, A. M. LaChance, S. Zeng, B. Liu and L. Sun, Synthesis, properties, and applications of graphene oxide/reduced graphene oxide and their nanocomposites, *Nano Mater. Sci.*, 2019, **1**, 31–47, DOI: 10.1016/j.nanoms.2019.02.004.

22 T. Y. Huang, C. W. Kung, H. Y. Wei, K. M. Boopathi, C. W. Chu and K. C. Ho, A high performance electrochemical sensor for acetaminophen based on a rGO-PEDOT nanotube composite modified electrode, *J. Mater. Chem. A*, 2014, **2**, 7229–7237, DOI: 10.1039/c4ta00309h.

23 Ö. A. Yokuş, F. Kardaş, O. Akyildirim, T. Eren, N. Atar and M. L. Yola, Sensitive voltammetric sensor based on polyoxometalate/reduced graphene oxide nanomaterial: application to the simultaneous determination of l-tyrosine and l-tryptophan, *Sens. Actuators, B*, 2016, **233**, 47–54, DOI: 10.1016/j.snb.2016.04.050.

24 A. A. Abraham, M. Rezayi, N. S. A. Manan, L. Narimani, A. N. Bin Rosli and Y. Alias, A novel potentiometric sensor based on 1,2-bis(*N*′-benzoylthioureido)benzene and reduced graphene oxide for determination of lead(II) cation in raw milk, *Electrochim. Acta*, 2015, **165**, 221–231, DOI: 10.1016/j.electacta.2015.03.003.

25 F. A. Harraz, M. Faisal, A. A. Ismail, S. A. Al-Sayari, A. E. Al-Salami, A. Al-Hajry and M. S. Al-Assiri, TiO_2/reduced graphene oxide nanocomposite as efficient ascorbic acid amperometric sensor, *J. Electroanal. Chem.*, 2019, **832**, 225–232, DOI: 10.1016/j.jelechem.2018.11.004.

26 A. Benvidi, N. Rajabzadeh, M. Mazloum-Ardakani, M. M. Heidari and A. Mulchandani, Simple and label-free electrochemical impedance Amelogenin gene hybridization biosensing based on reduced graphene oxide, *Biosens. Bioelectron.*, 2014, **58**, 145–152, DOI: 10.1016/j.bios.2014.01.053.

27 M. Z. H. Khan, X. Liu, J. Zhu, F. Ma, W. Hu and X. Liu, Electrochemical detection of tyramine with ITO/APTES/ErGO electrode and its application in real sample analysis, *Biosens. Bioelectron.*, 2018, **108**, 76–81, DOI: 10.1016/j.bios.2018.02.042.

28 M. Yadav, V. Ganesan, R. Gupta, D. K. Yadav and P. K. Sonkar, Cobalt oxide nanocrystals anchored on graphene sheets for electrochemical determination of chloramphenicol, *Microchem. J.*, 2019, **146**, 881–887, DOI: 10.1016/j.microc.2019.02.025.

29 M. Govindasamy, S. F. Wang, S. Kumaravel, R. J. Ramalingam and H. A. Al-lohedan, Facile synthesis of copper sulfide decorated reduced graphene oxide nanocomposite for high sensitive detection of toxic antibiotic in milk, *Ultrason. Sonochem.*, 2019, **52**, 382–390, DOI: 10.1016/j.ultsonch.2018.12.015.

30 J. Sethi, M. Van Bulck, A. Suhail, M. Safarzadeh, A. Perez-Castillo and G. Pan, A label-free biosensor based on graphene and reduced graphene oxide dual-layer for electrochemical determination of beta-amyloid biomarkers, *Microchim. Acta*, 2020, **187**, 1–10, DOI: 10.1007/s00604-020-04267-x.

31 S. Roy, N. Soin, R. Bajpai, D. S. Misra, J. A. McLaughlin and S. S. Roy, Graphene oxide for electrochemical sensing applications, *J. Mater. Chem.*, 2011, **21**, 14725–14731, DOI: 10.1039/c1jm12028j.

32 S. Guo and E. Wang, Synthesis and electrochemical applications of gold nanoparticles, *Anal. Chim. Acta*, 2007, **598**, 181–192, DOI: 10.1016/j.aca.2007.07.054.

33 A. K. Suresh, D. A. Pelletier, W. Wang, M. L. Broich, J. W. Moon, B. Gu, D. P. Allison, D. C. Joy, T. J. Phelps and M. J. Doktycz, Biofabrication of discrete spherical gold nanoparticles using the metal-reducing bacterium *Shewanella oneidensis*, *Acta Biomater.*, 2011, **7**, 2148–2152, DOI: 10.1016/j.actbio.2011.01.023.

34 S. L. Smitha and K. G. Gopchandran, Surface enhanced Raman scattering, antibacterial and antifungal active triangular gold nanoparticles, *Spectrochim. Acta, Part A*, 2013, **102**, 114–119, DOI: 10.1016/j.saa.2012.09.055.

35 J. Hernández, J. Solla-Gullón, E. Herrero, A. Aldaz and J. M. Feliu, Electrochemistry of shape-controlled catalysts: oxygen reduction reaction on cubic gold nanoparticles, *J. Phys. Chem. C*, 2007, **111**, 14078–14083, DOI: 10.1021/jp0749726.

36 H. Liu, N. Pierre-Pierre and Q. Huo, Dynamic light scattering for gold nanorod size characterization and study of nanorod-protein interactions, *Gold Bull.*, 2012, **45**, 187–195, DOI: 10.1007/s13404-012-0067-4.

37 Y. Jiang, X.-J. Wu, Q. Li, J. Li and D. Xu, Facile synthesis of gold nanoflowers with high surface-enhanced Raman scattering activity, *Nanotechnology*, 2011, **22**, 385601, DOI: 10.1088/0957-4484/22/38/385601.

38 S. He, Y. Ma, J. Zhou, J. Zeng, X. Liu, Z. Huang, X. Chen and X. Chen, A direct "touch" approach for gold nanoflowers decoration on graphene/ionic liquid composite modified electrode with good properties for sensing bisphenol A, *Talanta*, 2019, **191**, 400–408, DOI: 10.1016/j.talanta.2018.08.093.

39 Z. Luo, Q. Qi, L. Zhang, R. Zeng, L. Su and D. Tang, Branched polyethylenimine-modified upconversion nanohybrid-

mediated photoelectrochemical immunoassay with synergistic effect of dual-purpose copper ions, *Anal. Chem.*, 2019, **91**, 4149–4156, DOI: 10.1021/acs.analchem.8b05959.

40 R. Zeng, Z. Luo, L. Su, L. Zhang, D. Tang, R. Niessner and D. Knopp, Palindromic Molecular Beacon Based Z-Scheme BiOCl–Au–CdS Photoelectrochemical Biodetection, *Anal. Chem.*, 2019, **91**, 2447–2454, DOI: 10.1021/acs.analchem.8b05265.

41 S. Xu, B. Dai, J. Xu, L. Jiang and H. Huang, An Electrochemical Sensor for the Detection of Cu^{2+} Based on Gold Nanoflowers-modified Electrode and DNAzyme Functionalized Au@MIL-101 (Fe), *Electroanalysis*, 2019, **31**, 2330–2338, DOI: 10.1002/elan.201900343.

42 Y. C. Gao, K. Xi, W. N. Wang, X. D. Jia and J. J. Zhu, A novel biosensor based on a gold nanoflowers/hemoglobin/carbon nanotubes modified electrode, *Anal. Methods*, 2011, **3**, 2387–2391, DOI: 10.1039/c1ay05378g.

43 C. Hu, J. Deng, X. Xiao, X. Zhan, K. Huang, N. Xiao and S. Ju, Determination of dimetridazole using carbon paste electrode modified with aluminum doped surface molecularly imprinted siloxane, *Electrochim. Acta*, 2015, **158**, 298–305, DOI: 10.1016/j.electacta.2015.01.176.

44 M. Bakar, A. Morshed, F. Islam and R. Karim, Screening of chloramphenicol residues in chickens and fish in Chittagong city of Bangladesh, Bangladesh, *J. Vet. Med.*, 2014, **11**, 173–175, DOI: 10.3329/bjvm.v11i2.19144.

45 S. Gurunathan, J. W. Han, J. H. Park and J. H. Kim, A green chemistry approach for synthesizing biocompatible gold nanoparticles, *Nanoscale Res. Lett.*, 2014, **9**, 1–11, DOI: 10.1186/1556-276X-9-248.

46 S. Ahn, P. Singh, M. Jang, Y. J. Kim, V. Castro-Aceituno, S. Y. Simu, Y. J. Kim and D. C. Yang, Gold nanoflowers synthesized using Acanthopanacis cortex extract inhibit inflammatory mediators in LPS-induced RAW264.7 macrophages *via* NF-κB and AP-1 pathways, *Colloids Surf., B*, 2018, **162**, 398–404, DOI: 10.1016/j.colsurfb.2017.11.037.

47 M. Z. H. Khan, M. Daizy, C. Tarafder and X. Liu, Au-PDA@SiO_2 core–shell nanospheres decorated rGO modified electrode for electrochemical sensing of cefotaxime, *Sci. Rep.*, 2019, **9**, DOI: 10.1038/s41598-019-55517-9.

48 H. Peng, B. Pan, M. Wu, Y. Liu, D. Zhang and B. Xing, Adsorption of ofloxacin and norfloxacin on carbon nanotubes: hydrophobicity- and structure-controlled process, *J. Hazard. Mater.*, 2012, 233–234, DOI: 10.1016/j.jhazmat.2012.06.058.

49 W. Yi, Z. Li, C. Dong, H. W. Li and J. Li, Electrochemical detection of chloramphenicol using palladium nanoparticles decorated reduced graphene oxide, *Microchem. J.*, 2019, **148**, 774–783, DOI: 10.1016/j.microc.2019.05.049.

50 Y.-M. Xia, W. Zhang, M.-Y. Li, M. Xia, L.-J. Zou and W.-W. Gao, Effective Electrochemical Determination of Chloramphenicol and Florfenicol Based on Graphene/Copper Phthalocyanine Nanocomposites Modified Glassy Carbon Electrode, *J. Electrochem. Soc.*, 2019, **166**, B654–B663, DOI: 10.1149/2.0801908jes.

51 R. Karthik, M. Govindasamy, S. M. Chen, V. Mani, B. S. Lou, R. Devasenathipathy, Y. S. Hou and A. Elangovan, Green synthesized gold nanoparticles decorated graphene oxide for sensitive determination of chloramphenicol in milk, powdered milk, honey and eye drops, *J. Colloid Interface Sci.*, 2016, **475**, 46–56, DOI: 10.1016/j.jcis.2016.04.044.

52 K. Giribabu, S. C. Jang, Y. Haldorai, M. Rethinasabapathy, S. Y. Oh, A. Rengaraj, Y. K. Han, W. S. Cho, C. Roh and Y. S. Huh, Electrochemical determination of chloramphenicol using a glassy carbon electrode modified with dendrite-like Fe_3O_4 nanoparticles, *Carbon Lett.*, 2017, **23**, 38–47, DOI: 10.5714/CL.2017.23.038.

53 N. Yalikun, X. Mamat, Y. Li, X. Hu, T. Wågberg, Y. Dong and G. Hu, Synthesis of an iron–nitrogen co-doped ordered mesoporous carbon–silicon nanocomposite as an enhanced electrochemical sensor for sensitive and selective determination of chloramphenicol, *Colloids Surf., B*, 2018, **172**, 98–104, DOI: 10.1016/j.colsurfb.2018.08.011.

54 T. Sun, H. Pan, Y. Mei, P. Zhang, D. Zeng, X. Liu, S. Rong and D. Chang, Electrochemical sensor sensitive detection of chloramphenicol based on ionic-liquid-assisted synthesis of de-layered molybdenum disulfide/graphene oxide nanocomposites, *J. Appl. Electrochem.*, 2019, **49**, 261–270, DOI: 10.1007/s10800-018-1271-6.

55 M. Govindasamy, S. M. Chen, V. Mani, R. Devasenathipathy, R. Umamaheswari, K. Joseph Santhanaraj and A. Sathiyan, Molybdenum disulfide nanosheets coated multiwalled carbon nanotubes composite for highly sensitive determination of chloramphenicol in food samples milk, honey and powdered milk, *J. Colloid Interface Sci.*, 2017, **485**, 129–136, DOI: 10.1016/j.jcis.2016.09.029.